## Enhancing Optomechanical Entanglement and Mechanical Squeezing by the Synergistic Effect of Quadratic Optomechanical Coupling and Coherent Feedback

Ya-Feng Jiao, <sup>1,2,3,\*</sup> Ruo-Chen Wang, <sup>1</sup> Jing-Xue Liu, <sup>4</sup> Hui-Lai Zhang, <sup>1,2,3</sup> Ya-Chuan Liang, <sup>1,2,3</sup> Yan Wang, <sup>1,2,3</sup> Le-Man Kuang, <sup>5,2</sup> and Hui Jing <sup>5,2,6</sup>

School of Electronics and Information, Zhengzhou University of Light Industry, Zhengzhou 450001, P.R.China
 Academy for Quantum Science and Technology, Zhengzhou University of Light Industry, Zhengzhou 450001, P.R.China
 <sup>3</sup>Henan Key Laboratory of Information Functional Materials and Sensing Technology, Zhengzhou University of Light Industry, Zhengzhou 450001, P.R.China
 <sup>4</sup>School of Physics, Henan Normal University, Xinxiang 453007, China
 <sup>5</sup>Key Laboratory of Low-Dimensional Quantum Structures and Quantum Control of Ministry of Education, Department of Physics and Synergetic Innovation Center for Quantum Effects and Applications, Hunan Normal University, Changsha 410081, China
 <sup>6</sup>Institute for Quantum Science and Technology, College of Science, NUDT, Changsha 410073, P.R.China (Dated: October 7, 2025)

Quantum entanglement and squeezing associated with the motions of massive mechanical oscillators play an essential role in both fundamental science and emerging quantum technologies, yet realizing such macroscopic nonclassical states remains a formidable challenge. In this paper, we investigate how to achieve strong optomechanical entanglement and mechanical squeezing in a membrane-embedded cavity optomechanical system incorporating a coherent feedback loop, where the membrane interacts with the cavity mode through both linear and quadratic optomechanical couplings. This hybrid optomechanical architecture offers a flexible tunability of intrinsic system parameters, thus allowing the membrane to be stiffened or softened through tuning the sign of quadratic optomechanical coupling and the cavity decay rate to be reduced via feedback control. Exploiting these unique features, we demonstrate that optomechanical entanglement can be substantially enhanced with positive coupling sign and suitable feedback parameters, while strong mechanical squeezing beyond the 3dB limit is simultaneously achieved over a broad parameter range with negative coupling sign, reaching squeezing degree above 10dB under optimized conditions. Our proposal, establishing an all-optical method for generating highly entangled or squeezed states in cavity optomechanical systems, opens up a new route to explore macroscopic quantum effects and to advance quantum information processing.

### I. INTRODUCTION

Quantum entanglement [1] and squeezing [2], as striking features of quantum mechanics, have attracted intense interests owing to their potential applications in modern quantum science and technologies [3]. In particular, the preparation of entangled or squeezed states in massive mechanical systems has long been an ongoing pursuit [4, 5], which is not only because of their great significance for the fundamental tests of quantum theory and the exploration of the classical-quantum boundary [6], but also because such states can provide indispensable resources for advancing quantum technologies beyond the classical limits, e.g., improving sensitivity in ultraprecision measurement [7], enhancing security in communication [8], and boosting computational efficiency in information processing [9]. Nevertheless, the generation and preservation of such macroscopic nonclassical states are severely hindered by the decoherence effect induced by environmental thermal noise. In the past decades, a lot of effort has been devoted both theoretically and experimentally to overcome this difficulty, leading to a variety of schemes for realizing macroscopic entanglement [10–12] and squeezing [13– 15]. For instance, entanglement generation has been explored via injection of quantum squeezing [16–18] or synthetic gauge

fields [19–21], dark-mode [22, 23] or feedback control [24–26], photon counting [27], dynamical modulation [28–30], and nonreciprocal manipulation [31–33], while mechanical squeezing has been pursued through using frequency modulation [34–36], monochromatic driving [37, 38], backaction-evading measurements [39–41], dark-mode [42] or feedback control [43, 44], and reservoir engineering [45–47].

On the other hand, cavity optomechanical (COM) systems [48], capable of cooling massive mechanical oscillators to their ground state [49–51], have emerged as a versatile platform for exploring a wide range of nonclassical effects [52], including single-photon or single-phonon blockade [53–56], quantum phase transitions [57], quantum chaos [58], photonphonon coherent conversion [59, 60], and optomechanical Bell tests [61], to name a few. In a recent experiment, nonclassical correlations were even produced between light and 40 kg mirrors [62], showing a joint quantum uncertainty below the standard quantum limit. A closely related research topic to the present study is the generation and manipulation of macroscopic entanglement [63-65] and squeezing [66-68] involving massive mechanical oscillators. Recently, by exploiting the down-conversion interaction enabled by the radiationpressure-induced nonlinear COM coupling [48, 52], remarkable progresses have been made towards the observation of quantum entanglement between light and motion [69, 70], between propagating optical fields [71, 72], and between massive mechanical oscillators [73-76]. Meanwhile, numerous schemes for generating strong optical and mechani-

<sup>\*</sup> yfjiao@zzuli.edu.cn

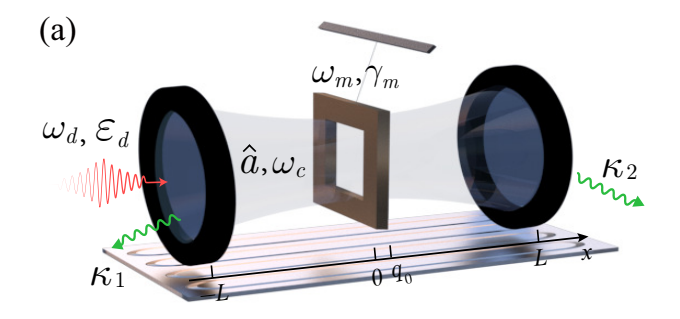
cal squeezing beyond the 3dB limit have been theoretically reported [77–79] and experimentally demonstrated [80–82], which provide an effective means to reduce the system fluctuations below the standard quantum limit. Particularly, recent studies have shown that COM systems with both linear (LOC) and quadratic (QOC) optomechanical couplings [49] exhibit a static mechanical response that is highly sensitive to the sign of the QOC interaction [83], thereby enabling the improvement of mechanical squeezing and cooling [84], optical harmonic generation [85], and optomechanical entanglement.

Inspired by these studies, we here investigate how to achieve strong COM entanglement and mechanical squeezing through coupling a COM system that supports both LOC and QOC to a coherent feedback loop. By harnessing the interplay of QOC and coherent feedback, it is shown that the fundamental mechanical frequency and cavity decay rate become tunable, thus providing a powerful tool for quantum engineering. Exploiting this feature, it is further found that COM entanglement can be considerably enhanced for positive QOC with suitable feedback parameters, reaching an enhancement factor of about 5 under optimized conditions. In addition, strong mechanical squeezing beyond the 3dB limit is simultaneously achieved for negative QOC, with optimal squeezing degrees exceeding 10dB under proper feedback parameters. Overall, our proposed scheme, showcasing the transformative potential for engineering and improving various nonclassical effects involving massive mechanical systems [53–61], are expected to advance a wide range of COM-based applications [3, 48, 52] ranging from quantum sensing [7] to quantum networking [8, 59] and quantum computing [9].

This paper is structured as follows. In Sec. II, we introduce the theoretical model of the proposed COM system and derive the effective Hamiltonian, on the basis of which the system dynamics and the quantitative measures of COM entanglement and mechanical squeezing are obtained. In Secs. III and IV, we present the numerical simulations of the behavior of COM entanglement and mechanical squeezing under various controlling parameters, and analyze the underlying physical mechanism. In Sec. V, we provide a brief summary of the main results.

#### II. THEORETICAL MODEL

As shown in Fig. 1(a), we consider a hybrid COM system consisting of a Fabry-Perot (FP) cavity and a membrane with finite reflectivity  $R_m$ . The FP cavity is formed by two fixed mirrors located at positions  $x=\pm L$ , and the membrane, with its thickness much smaller than the optical wavelength, is placed inside the cavity at an equilibrium position  $x=q_0$ . In this configuration, the mode frequencies of the FP cavity and the type of optomechanical interactions are determined by the value of  $R_m$  and  $q_0$ . On one hand, in the case of  $R_m=1$  and  $R_m=1$ 0, the FP cavity is effectively divided into two subcavities, supporting two-fold degenerate optical modes at frequency  $R_m=1$ 0, where  $R_m=1$ 1 is the mode number, and  $R_m=1$ 2 is the speed of light,  $R_m=1$ 3 is the mode number, and  $R_m=1$ 4 in the other



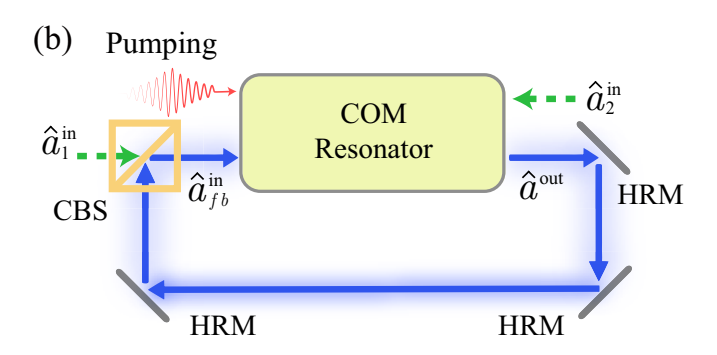


FIG. 1. Schematic diagram of a membrane-embedded COM system coupled with a coherent feedback loop. (a) The COM system comprises a FP cavity formed by two fixed mirrors with optical decay rates  $\kappa_1$  and  $\kappa_2$ , inside which a partially reflecting membrane with reflectivity  $R_m$  is located near the cavity center. The FP cavity with resonance frequency  $\omega_c$  is driven by a coherent laser field of frequency  $\omega_d$  and amplitude  $\varepsilon_d$ . The membrane, characterized by resonance frequency  $\omega_m$  and damping rate  $\gamma_m$ , couples to the cavity mode through both linear  $(g_1)$  and quadratic  $(g_2)$  optomechanical couplings. (b) The coherent feedback loop consists of three highly reflected mirrors (HRMs) and a controllable beam splitter (CBS) with tunable reflection coefficient  $r_B$ . The blue arrows indicate that the optical output field  $\hat{a}^{\text{out}}$  transmitted from the right-hand mirror are fed back to the cavity through the left-hand mirror.  $\hat{a}_1^{\text{in}}$  and  $\hat{a}_2^{\text{in}}$ describe the optical input noise arising from the zero-point fluctuations in the vacuum entering the cavity from the CBS and the righthand mirror.

hand, when  $R_m \neq 1$  and  $q_0 \neq 0$ , the optical degeneracy of the two subcavity modes is lifted, yielding a pair of nondegenerate modes at frequencies  $\omega_{n,e}$  and  $\omega_{n,o}$ , which correspond to the even and odd half-wavelength modes of the full FP cavity, respectively. For large mode numbers with  $L \gg \lambda_n$ and  $q_0 \ll \lambda_n$ , although both subcavity modes couple to the same membrane, there is no photon scattering between them via the membrane, as the membrane's mechanical frequency  $\omega_m$  is much smaller than the two subcavities' optical frequencies in this case. In this case, when the membrane is placed near the middle of the cavity (i.e.,  $q_0 \approx 0$ , near an antinode), the cavity resonance frequency is primarily dominated by  $\omega_{n,o}$  of the odd half-wavelength modes. For a sufficiently small value of  $\omega_m$ , i.e.,  $\omega_m \ll 1/\tau$  (with  $\tau = 2L/c$  the round trip time of light for each subcavity), the cavity resonance frequency  $\omega_{n,o}$  follows the membrane motion adiabatically, and it can be simply parameterized by the membrane position  $q_1$ ,

which is given by [86]

$$\omega_{n,o}(q_1) \simeq \omega_n + \frac{\pi}{\tau} - \frac{1}{\tau} \left\{ \sin^{-1} [\sqrt{R_m} \cos(2k_n q_1)] + \sin^{-1} (\sqrt{R_m}) \right\},$$
 (1)

where  $k_n = \omega_n/c$ . Given that the equilibrium position  $q_0$  of the membrane is small, we expand  $\omega_{n,o}(q_1)$  in powers of  $q_0$  up to the second order,

$$\omega_{n,o}(q_1) = \omega_{n,o}(q_0) + \frac{d\omega_{n,o}(q_1)}{dq_1} \Big|_{q_1 = q_0} (q_1 - q_0)$$

$$+ \frac{1}{2} \frac{d^2\omega_{n,o}(q_1)}{dq_1^2} \Big|_{q_1 = q_0} (q_1 - q_0)^2$$

$$= \omega_c + g_1 q + g_2 q^2, \tag{2}$$

with

$$\omega_{c} = \omega_{n,o}(q_{0}),$$

$$g_{1} = \frac{2k_{n}}{\tau\sigma} \sqrt{R_{m}} \sin(2k_{n}q_{0}),$$

$$g_{2} = \frac{2k_{n}^{2}}{\tau\sigma^{3}} \sqrt{R_{m}} (1 - R_{m}) \cos(2k_{n}q_{0}),$$

$$\sigma = \sqrt{\sin^{2}(2k_{n}q_{0}) + (1 - R_{m}) \cos^{2}(2k_{n}q_{0})},$$
(3)

where  $q=q_1-q_0$  is the displacement of the membrane from its equilibrium position. Equations (2) and (3) indicate that when the membrane is placed in the middle of the cavity (i.e.,  $q_0=0$ ), the optomechanical coupling is purely quadratic, with  $g_1=0$  and  $g_2\neq 0$ . In contrast, when the membrane has a slight mechanical displacement from the middle (i.e.,  $q_0\approx 0$ ), both linear and quadratic optomechanical couplings are present, with  $g_1\neq 0$  and  $g_2\neq 0$ . In this paper, we focus on the latter case for two reasons: (i) our work aims to investigate the role of QOC in enhancing optomechanical entanglement and mechanical squeezing, and (ii) placing the membrane exactly at the middle of the cavity is experimentally challenging in practice. Accordingly, the Hamiltonian of this optomechanical system reads

$$H = \hbar \omega_c \hat{a}^{\dagger} \hat{a} + \frac{\hbar \omega_m}{2} (\hat{p}^2 + \hat{q}^2) - \hbar g_1 \hat{a}^{\dagger} \hat{a} \hat{q} - \hbar g_2 \hat{a}^{\dagger} \hat{a} \hat{q}^2$$
$$+ i\hbar E_d (e^{-i\omega_0 t} \hat{a}^{\dagger} - e^{i\omega_0 t} \hat{a}), \tag{4}$$

where  $\hat{a}$  ( $\hat{a}^{\dagger}$ ) denotes the annihilation (creation) operator of the cavity mode, and  $\hat{q}$  and  $\hat{p}$  are the dimensionless position and momentum operators of the membrane, respectively. In Eq. (4), the first two terms correspond to the free Hamiltonians of the cavity and the mechanical modes, respectively. The third and fourth terms describe the linear and quadratic couplings between the cavity and the membrane, with coupling strengths  $g_1$  and  $g_2$  [see Eq. (3)]. The last term is the Hamiltonian of the coherent driving field with amplitude  $\varepsilon_d$  and frequency  $\omega_d$ .  $\varepsilon_d$  is related to the input laser power  $P_d$  by  $|\varepsilon_d| = \sqrt{2P_d\kappa_1/\hbar\omega_d}$ , with  $\kappa_1$  the cavity decay rate due to optical transmission through the left-hand mirror.

By considering the system dissipations and environmental input noises, the dynamical evolution of this COM system can be fully characterized by the quantum Langevin equations (QLEs):

$$\dot{\hat{q}} = \omega_{m}\hat{p}, 
\dot{\hat{p}} = -\omega_{m}\hat{q} - \gamma_{m}\hat{p} + g_{1}\hat{a}^{\dagger}\hat{a} + 2g_{2}\hat{a}^{\dagger}\hat{a}\hat{q} + \hat{\xi}, 
\dot{\hat{a}} = -(i\Delta_{c} + \kappa_{1} + \kappa_{2})\hat{a} + ig_{1}\hat{a}\hat{q} + ig_{2}\hat{a}\hat{q}^{2} + \varepsilon_{d} 
+ \sqrt{2\kappa_{1}}\hat{a}_{1}^{\text{in}} + \sqrt{2\kappa_{2}}\hat{a}_{2}^{\text{in}},$$
(5)

where  $\Delta_c = \omega_c - \omega_d$ ,  $\gamma_m$  denotes the mechanical damping rate, and  $\kappa_2$  denotes the cavity decay rate of the right-hand mirror.  $\hat{a}_1^{\text{in}}$  and  $\hat{a}_2^{\text{in}}$  describe the optical input noise arising from the zero-point fluctuations in the vacuum entering the cavity from the CBS and the right-hand mirror, which have zero mean and are characterized by the following nonvanishing correlation function [87]:  $\langle \hat{a}_{j}^{\rm in}(t)\hat{a}_{j}^{\rm in,\dagger}(t')\rangle = \delta(t-t')$ , with j=1,2.  $\hat{\xi}$  is the Brownian thermal noise operator, which describes the stochastic Brownian force acting on the membrane. The correlation function of  $\hat{\xi}$  is typically not delta-correlated, i.e.,  $\langle \hat{\xi}(t)\hat{\xi}(t')\rangle = \frac{\gamma_m}{\omega_m}\int \frac{d\omega}{2\pi} \mathrm{e}^{-\mathrm{i}\omega(t-t')}\omega[\coth(\frac{\hbar\omega}{2k_\mathrm{B}T})+1]$ , which describes a non-Markovian process. However, for high-Q mechanical membranes, i.e.,  $Q_m = \omega_m/\gamma_m \gg 1$ , one can safely make the Markovian approximation and the correlation function of  $\hat{\xi}$  can be reduced to a delta-correlated form [87]:  $\langle \hat{\xi}(t)\hat{\xi}(t')\rangle \simeq \gamma_m(2n_m+1)\delta(t-t')$ , where  $n_m = [\exp(\hbar\omega_m/k_BT)-1]^{-1}$  is the equilibrium mean thermal phonon number, with  $k_B$  the Boltzmann constant and Tthe bath temperature.

The dynamics of QLEs (5) involve radiation-pressure-induced nonlinear COM interactions between the cavity field and the membrane, and thus are difficult to be directly solved. In order to find solutions to QLEs (5), one can linearize the system dynamics under a sufficiently strong driving condition by expanding each operator as a sum of its steady-state mean value and a quantum fluctuation around it:  $\hat{a} = \alpha_s + \delta \hat{a}$ ,  $\hat{q} = q_s + \delta \hat{q}$ ,  $\hat{p} = p_s + \delta \hat{p}$ . Inserting this assumption into the QLEs (5) yields a set of nonlinear algebraic equations for the steady-state mean values and a set of linearized QLEs for the fluctuation operators. By solving the nonlinear algebraic equations, the steady-state mean values are obtained as

$$p_{s} = 0,$$

$$q_{s} = \frac{g_{1}|\alpha_{s}|^{2}}{\omega_{m} - 2g_{2}|\alpha_{s}|^{2}},$$

$$\alpha_{s} = \frac{\varepsilon_{d}}{i\overline{\Delta} + \kappa_{1} + \kappa_{2}},$$
(6)

where

$$\bar{\Delta} = \Delta_c - g_1 q_s - g_2 q_s^2 \tag{7}$$

is the effective optical detuning including optomechanical frequency shift. Furthermore, by neglecting the high-order terms in the QLEs for fluctuation operators, i.e.,  $\delta \hat{a}^{\dagger} \delta \hat{a}$ ,  $\delta \hat{a}^{\dagger} \delta \hat{q}$ ,  $\delta \hat{a} \delta \hat{q}$ ,

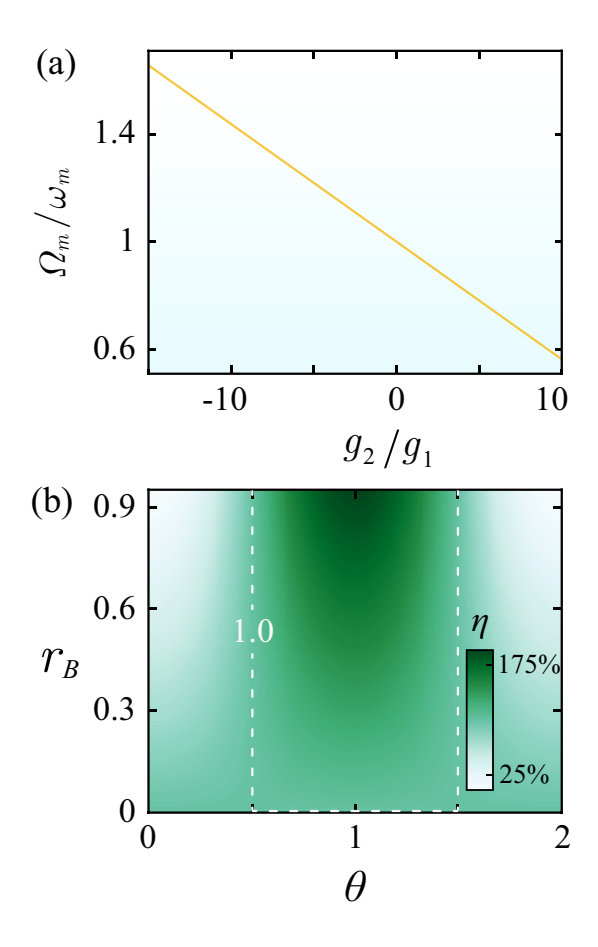


FIG. 2. The influence of QOC and coherent feedback on system parameters. (a) The effective membrane frequency  $\Omega_m$  versus the dimensionless QOC strength  $g_2/g_1$ . When changing the sign of QOC,  $\Omega_m$  increases for  $g_2 < 0$  and decreases for  $g_2 > 0$ , which thus provides an efficient method for manipulating quantum effect. (b) The decay ratio  $\eta$ , characterizing the reduction efficiency of the cavity decay rate, is plotted as a function of the feedback parameters  $r_B$  and  $\theta$ . By properly adjusting  $r_B$  and  $\theta$ ,  $\eta$  is effectively reduced, leading to a significant suppression of cavity decay rate. The parameters used here are provided in the main text.

 $\delta \hat{q} \delta \hat{q}$ , and  $\delta \hat{a}^{\dagger} \delta \hat{a} \delta \hat{q}$ , the linearized QLEs are derived as

$$\begin{split} \delta \dot{q} &= \omega_m \delta \hat{p}, \\ \delta \dot{\hat{p}} &= -\Omega_m \delta \hat{q} - \gamma_m \delta \hat{p} + \lambda (\delta \hat{a} + \delta \hat{a}^{\dagger}) + \hat{\xi}, \\ \delta \dot{\hat{a}} &= - (i\bar{\Delta} + \kappa_1 + \kappa_2) \delta \hat{a} + i\lambda \delta \hat{q} + \sqrt{2\kappa_1} \hat{a}_1^{\text{in}} + \sqrt{2\kappa_2} \hat{a}_2^{\text{in}}, \end{split}$$
(8)

where  $\Omega_m=\omega_m-2g_2|\alpha_s|^2$  is the effective membrane frequency, and  $\lambda=(g_1+2g_2q_s)\alpha_s$  denote the effective COM coupling strength. Here  $\alpha_s$  is assumed to be real by choosing a suitable phase reference for the cavity field. As shown in Fig. 2(a), the effective membrane frequency  $\Omega_m$  is sensitive to the sign of QOC strength  $g_2$ , namely,  $\Omega_m$  is enhanced for  $g_2<0$  and is suppressed for  $g_2>0$ , implying that the membrane becomes either stiffer or softer depending on the sign of  $g_2$ . This tunability provides a useful tool for the manipulation of quantum effects in this system.

When coupling a coherent feedback loop to the COM setup, as depicted in Fig. 1(b), the optical output field transmitted from the right-hand mirror can be sent back into the cavity through the left-hand mirror. By using the standard input-output relation, the output field is given by [88]

$$\hat{a}^{\text{out}} = \sqrt{2\kappa_2}\delta\hat{a} - \hat{a}_2^{\text{in}}.$$
 (9)

Note that, since both cavity mirrors are fixed and the membrane is placed inside the cavity, the feedback process remains unaffected by the membrane's oscillation. Moreover, when the optical path between the two mirrors (loop length) is relatively short, the associated time delay of the output field becomes negligible compared with the cavity lifetime, so that the feedback process can be regarded as instantaneous. This is a good approximation for high-Q FP cavities. For example, as shown in Ref. [25], for a 5-cm FP cavity with a 10-cm feedback loop, the delay time is about  $10^{-10}$  s, which is much shorter than the typical cavity lifetime ( $\sim 10^{-7}$  s, corresponding to an optical Q-factor of  $\sim 10^6$ ). Accordingly, the new input field modified by the feedback can be modeled as the superposition of the original input noise and the returned output field, which are mixed in a lossless CBS before entering the cavity; the corresponding input field operator is given by

$$\hat{a}_{fb}^{\text{in}} = r_B \exp^{i\theta} \hat{a}^{\text{out}} + t_B \hat{a}_1^{\text{in}}, \tag{10}$$

where  $r_B$  and  $t_B$  denote the reflection and transmission coefficients of the CBS, with  $r_B^2 + t_B^2 = 1$ . The additional optical phase shift  $\theta$  of the output field accounts for the accumulated phase delay from light propagation in the feedback loop and is defined as  $\theta = 2\pi n L/\lambda$ , with n (L) the refractive index (length) of the loop and  $\lambda$  the light wavelength. Here we emphasize that the reflection coefficient  $r_B$  and additional optical phase shift  $\theta$  are defined in an effective way, such that they already account for optical losses and propagation-induced phase shifts in the feedback loop. As a result,  $r_B$  corresponds to the CBS reflectivity diminished by loop losses, implying that it can only approach, but never reach, unity ( $0 \le r_B < 1$ ).

Then, by replacing the bare input noise operator  $\hat{a}_1^{in}$  in Eq. (8) with the feedback-modified operator  $\hat{a}_{fb}^{in}$ , we obtain the QLE for the cavity mode in the presence of a coherent feedback loop as

$$\delta \dot{\hat{a}} = -(i\tilde{\Delta} + \tilde{\kappa})\delta \hat{a} + i\lambda \delta \hat{q} + \sqrt{2\,\tilde{\kappa}}\hat{A}^{\rm in},\tag{11}$$

where  $\tilde{\kappa} = \kappa_{\rm tot} - 2\sqrt{\kappa_1\kappa_2}r_B\cos\theta$  (with  $\kappa_{\rm tot} = \kappa_1 + \kappa_2$ ) and  $\tilde{\Delta} = \bar{\Delta} - 2\sqrt{\kappa_1\kappa_2}r_B\sin\theta$  are the feedback-modified effective cavity decay rate and detuning, respectively. Moreover, the feedback-modified input noise operator  $\hat{A}^{\rm in}$  is given by

$$\hat{A}^{\text{in}} = \frac{1}{\sqrt{\tilde{\kappa}}} \left[ \left( \sqrt{\kappa_2} - \sqrt{\kappa_1} r_B \exp^{i\theta} \right) \hat{a}_2^{\text{in}} + \sqrt{\kappa_1} t_B \hat{a}_1^{\text{in}} \right], \tag{12}$$

which corresponds to vacuum noise and obeys the correlation function:  $\langle \hat{A}^{\rm in}(t) \hat{A}^{\rm in\dagger}(t') \rangle = \delta(t-t')$ . Obviously, in the presence of coherent feedback, the cavity parameters  $\tilde{\kappa}$  and  $\tilde{\Delta}$  become tunable, which can either be enhanced or suppressed

by adjusting the feedback parameters  $r_B$  and  $\theta$ . In particular, as shown by the decay reduction ratio  $\eta \equiv \tilde{\kappa}/\kappa_{\rm tot}$  in Fig. 2(b), the effective cavity decay rate  $\tilde{\kappa}$  can be significantly reduced when  $\kappa_1 = \kappa_2$ , even reaching values below 25% of the original decay rate  $\kappa_{\rm tot}$ . This suppression in cavity decay is beneficial for enhancing entanglement and mechanical squeezing discussed below.

Accordingly, by introducing the optical quadrature operators  $\delta \hat{X} \equiv (\delta \hat{a}^\dagger + \delta \hat{a})/\sqrt{2}$  and  $\delta \hat{Y} \equiv i(\delta \hat{a}^\dagger - \delta \hat{a})/\sqrt{2}$ , together with the corresponding Hermitian input noise operators  $\hat{X}^{\rm in} \equiv (\hat{A}^{\rm in,\dagger} + \hat{A}^{\rm in})/\sqrt{2}$  and  $\hat{Y}^{\rm in} \equiv i(\hat{A}^{\rm in,\dagger} - \hat{A}^{\rm in})/\sqrt{2}$ , the feedback-modified linearized QLEs can be written in a compact form

$$\dot{u}(t) = A\hat{u}(t) + \hat{n}(t),\tag{13}$$

where

$$\hat{u}(t) = (\delta \hat{q}, \delta \hat{p}, \delta \hat{X}, \delta \hat{Y})^{T},$$

$$\hat{n}(t) = (0, \xi, \sqrt{2\tilde{\kappa}} \hat{X}^{\text{in}}, \sqrt{2\tilde{\kappa}} \hat{Y}^{\text{in}})^{T},$$
(14)

denote the vectors of quadrature fluctuations and input noises, respectively. The coefficient matrix A is given by

$$A = \begin{pmatrix} 0 & \omega_m & 0 & 0 \\ -\Omega_m & -\gamma_m & \sqrt{2}\lambda & 0 \\ 0 & 0 & -\tilde{\kappa} & \tilde{\Delta} \\ \sqrt{2}\lambda & 0 & \tilde{\Delta} & -\tilde{\kappa} \end{pmatrix}.$$
(15)

Owing to the linearized system dynamics and the Gaussian nature of the input noises, the steady state of the COM system, independently of any initial conditions, finally evolves into a zero-mean bipartite Gaussian state, which can be completely characterized by a  $4\times 4$  covariance matrix (CM) V with its entries defined as

$$V_{kl} = \langle \hat{u}_k(\infty) \hat{u}_l(\infty) + \hat{u}_l(\infty) \hat{u}_k(\infty) \rangle / 2,$$
  
$$k, l = 1, 2, 3, 4.$$
 (16)

The steady-state CM  ${\cal V}$  can be determined by solving the Lyapunov equation

$$AV + VA^{\mathsf{T}} = -D, (17)$$

where  $D = \text{Diag}\left[0, \gamma_m(2\bar{n}+1), \tilde{\kappa}, \tilde{\kappa}\right]$  is the diffusion matrix, and it is defined through  $D_{kl}\delta(s-s') = \langle \hat{n}_k(s)\hat{n}_l(s') + \hat{n}_l(s')\hat{n}_k(s)\rangle/2$ . The Lyapunov equation (17) is linear for V and can be solved straightforwardly; however, its general exact solution is cumbersome and will not be reported here.

# III. THE SYNERGISTIC EFFECT OF QOC AND COHERENT FEEDBACK ON STEADY-STATE OPTOMECHANICAL ENTANGLEMENT

Entanglement is a key resource for the implementation of various quantum information tasks, thus making its quantification an important problem. In continuous-variable (CV)

systems, entanglement can be certified by using different entanglement monotones, among which the logarithmic negativity  $E_{\mathcal{N}}$  is widely adopted as a quantitative entanglement measure. For bipartite CV Gaussian systems, the logarithmic negativity  $E_{\mathcal{N}}$  is defined as [89]

$$E_{\mathcal{N}} = \max[0, -\ln(2\nu^{-})],$$
 (18)

where  $\nu^- = 2^{-1/2} \{ \Sigma(V) - [\Sigma(V)^2 - 4 \det V]^{1/2} \}^{1/2}$  (with  $\Sigma(V) \equiv \det \mathcal{A} + \det \mathcal{B} - 2 \det \mathcal{C}$ ) is the minimum symplectic eigenvalue of the partial transpose of the CM V. Here we have rewritten the CM V in a  $2 \times 2$  block form

$$V = \begin{pmatrix} \mathcal{A} & \mathcal{C} \\ \mathcal{C}^T & \mathcal{B} \end{pmatrix}, \tag{19}$$

where the submatrices  $\mathcal{A}$  and  $\mathcal{B}$  describe the autocorrelations of the optical and mechanical modes, respectively, while the submatrix  $\mathcal{C}$  characterizes their cross-correlations. Equation (18) indicates that the optical and mechanical modes become entangled if and only if  $\nu^- < 1/2$ , in which case  $E_{\mathcal{N}}$  has a nonzero value. It should be emphasized that  $E_{\mathcal{N}}$  quantifies the extent to which the positivity of the partial transpose condition for separability is violated for the Gaussian state, which is equivalent to Simon's necessary and sufficient nonpositive partial transpose criterion (or the related Peres-Horodecki criterion) for bipartite entanglement.

Based on this measure, we now turn to examine the influence of QOC and coherent feedback on COM entanglement in Fig. 3. To this end, we numerically evaluate the steady-state CM V by solving Eq. (17) with the following experimental feasible parameters:  $\omega_m/2\pi=10\,\mathrm{MHz},\,\gamma_m/2\pi=100\,\mathrm{Hz},$  $\kappa_1/2\pi = \kappa_2/2\pi = 1.5 \,\text{MHz}, \, \lambda_d = 2\pi c/\omega_d = 810 \,\text{nm},$  $P_d=5\,\mathrm{mW},$  and  $T=10\,\mathrm{mK}.$  Note that, since our analysis focuses on the impact of QOC, we fix  $g_1 = 1351.38 \,\mathrm{Hz}$  and henceforth characterize the variation of  $g_2$  by a dimensionless QOC strength  $g_2/g_1$ . In Fig. 3(a), we first demonstrate the case without coherent feedback ( $r_B = 0$ ) by plotting the logarithmic negativity  $E_{\mathcal{N}}$  as a function of the scaled optical detuning  $\Delta/\omega_m$  for different values of  $g_2/g_1$ . In the absence of QOC, i.e.,  $g_2/g_1 = 0$ ,  $E_N$  is nonvanishing within a finite parameter region around detuning  $\Delta/\omega_m \simeq 0.6$ , which means the presence of bipartite COM entanglement between light and membrane. The slight spectral offset from the nominal COM resonance arises from the radiation-pressure-induced redshift of the cavity frequency [see the second term in Eq. 7]. On the other hand, in the presence of QOC with positive strength,  $E_N$  exhibits a sharp peak centered at  $\Delta/\omega_m \simeq 0.3$ and it decreases quickly after reaching its maximum value. Besides, larger positive values of  $g_2/g_1$  lead to enhanced maximum COM entanglement. For example, in the case of  $g_2/g_1 = 6 \times 10^{-5}$ , the maximum value of  $E_N$  is enhanced by approximately 3 times compared with the case of  $g_2/g_1 = 0$ . Physically, the further increased spectral offset is due to the cavity frequency shift induced by QOC [see the last term in Eq. 7]. Meanwhile, the enhancement of COM entanglement arises from the relaxation of the stability condition, which results from the softening of the membrane due to QOC [cf. the discussion of Fig. 2(a)]. This mechanism can be understood as

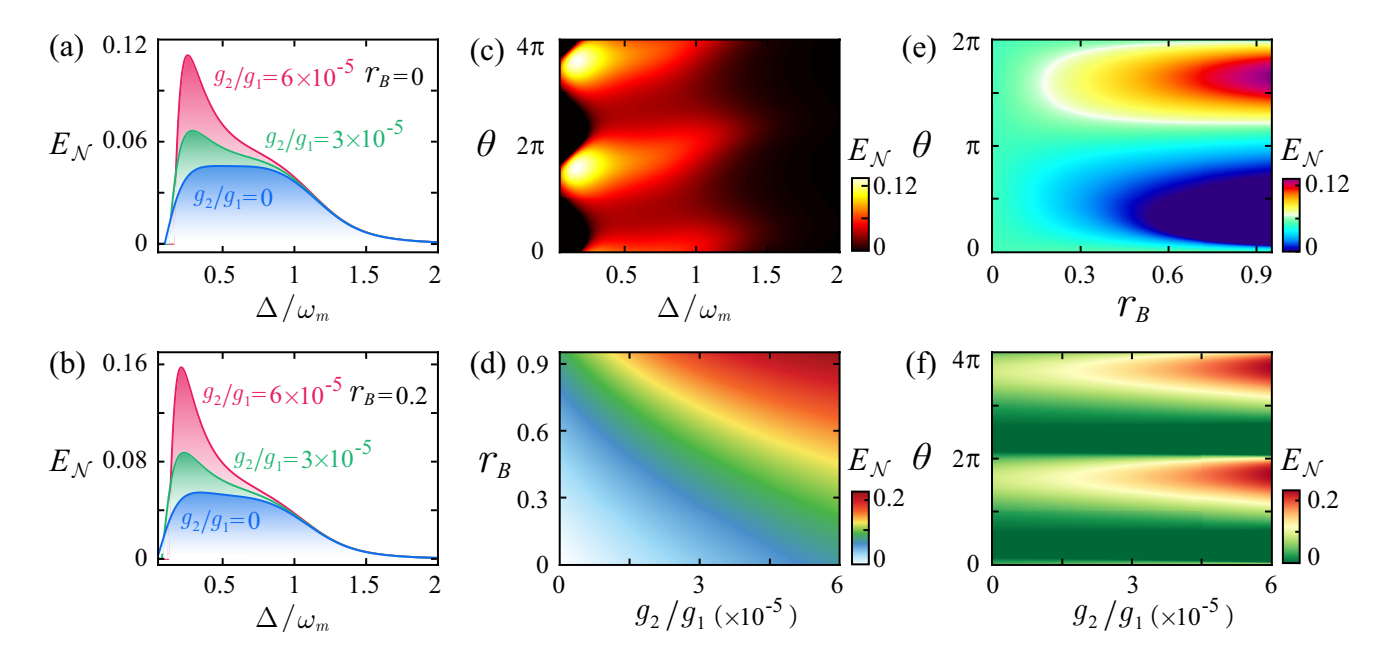


FIG. 3. Enhancement of optomechanical entanglement via the synergistic effect of QOC and coherent feedback. (a,b) The logarithmic negativity  $E_N$  versus the scaled optical detuning  $\Delta/\omega_m$  for different values of  $g_2/g_1$ : (a) without coherent feedback ( $r_B=0$ ) and (b) with coherent feedback ( $r_B=0.2$ ,  $\theta=3\pi/2$ ). (c-f) The logarithmic negativity  $E_N$  under different parameter settings: (c) as a function of the scaled optical detuning  $\Delta/\omega_m$  and optical phase shift  $\theta$  with  $r_B=0.5$  and  $g_2/g_1=3\times10^{-5}$ ; (d) as a function of the dimensionless QOC strength  $g_2/g_1$  and reflection coefficient  $r_B$  with  $\Delta/\omega_m=0.25$  and  $\theta=1.5\pi$ ; (e) as a function of the reflection coefficient  $r_B$  and optical phase shift  $\theta$  with  $\Delta/\omega_m=0.25$  and  $g_2/g_1=1.5\times10^{-5}$ ; (f) as a function of the dimensionless QOC strength  $g_2/g_1$  and optical phase shift  $\theta$  with  $\Delta/\omega_m=0.25$  and  $r_B=0.7$ . The other parameters are as in the main text.

follows. As discussed in Ref. [64], the stability of COM system relies on the balance between the radiation-pressure force and the mechanical restoring force, which imposes a threshold on  $E_{\mathcal{N}}$ , such that  $E_{\mathcal{N}}$  reaches its maximum near the instability point. When the membrane is softened  $(g_2 > 0)$ , this balance is relaxed, thereby broadening the stability regime and enabling stronger COM entanglement [90].

In Figs. 3(b)-3(f), we demonstrate the case with coherent feedback  $(r_B \neq 0)$ , where the interplay between QOC and feedback takes place. Compared with Fig. 3(a) and Fig. 3(b), one can intuitively find that, under the same QOC strength, a nonzero value of  $r_B$  (e.g.,  $r_B = 0.2$ ) leads to higher values of  $E_N$ , implying that COM entanglement can be further improved in the presence of coherent feedback. Moreover, as shown in Figs. 3(c)-3(f), we present the dependence of  $E_N$  on the controlling parameters  $r_B$ ,  $\theta$ ,  $g_2/g_1$ , and  $\Delta/\omega_m$ . From these results, it is found that the COM entanglement is further optimized by the controlling parameters, and this optimization is characterized by two generic features: (i)  $E_N$  increases monotonically with both  $r_B$  and  $g_2/g_1$ , confirming their cooperative role in enhancing COM entanglement; (ii)  $E_N$  shows a periodic dependence on the optical phase shift  $\theta$  with a period of  $2\pi$ , within which both maxima and minima occur. Here, compared with the result without feedback, the two extreme values are found to be either enhanced or suppressed, indicating that the synergistic control of QOC and feedback offers a flexible and efficient approach for generating and modulating COM entanglement. Moreover, the achievable maximum value of  $E_N$  can be above 0.2 under optimized condition [see Figs. 3(d) and 3(f)], which is about 5 times larger than that obtained without QOC and coherent feedback. Notably, this observed tunability of COM entanglement originates from the controllable behavior of the effective cavity decay rate. Specifically, as previously discussed in Fig. 2(b), when the reflection coefficient  $r_B$  increases, the effect of the optical phase shift  $\theta$  determines whether the decay is suppressed or amplified: for suitable values of  $\theta$ , the effective cavity decay rate decreases, leading to an enhancement of COM entanglement; whereas for unsuitable  $\theta$ , the decay rate increases, resulting in a suppression of COM entanglement.

# IV. THE SYNERGISTIC EFFECT OF QOC AND COHERENT FEEDBACK ON STEADY-STATE MECHANICAL SQUEEZING

The synergistic control of QOC and coherent feedback also provides a viable route to achieving strong mechanical squeezing beyond the 3dB limit. To quantify the squeezing of the membrane motion, we define the degree of squeezing as (in units of dB) [91]

$$S_j = -10\log_{10}\left(\frac{\sigma_j}{\sigma_{\rm zpf}}\right),\tag{20}$$

where  $\sigma_j$  (j=q,p) is the variance of the mechanical quadrature operator, obtained from the corresponding diagonal elements of the CM V, and  $\sigma_{\rm zpf}=|\langle[\delta\hat{q},\delta\hat{p}]\rangle|/2=1/2$  denotes

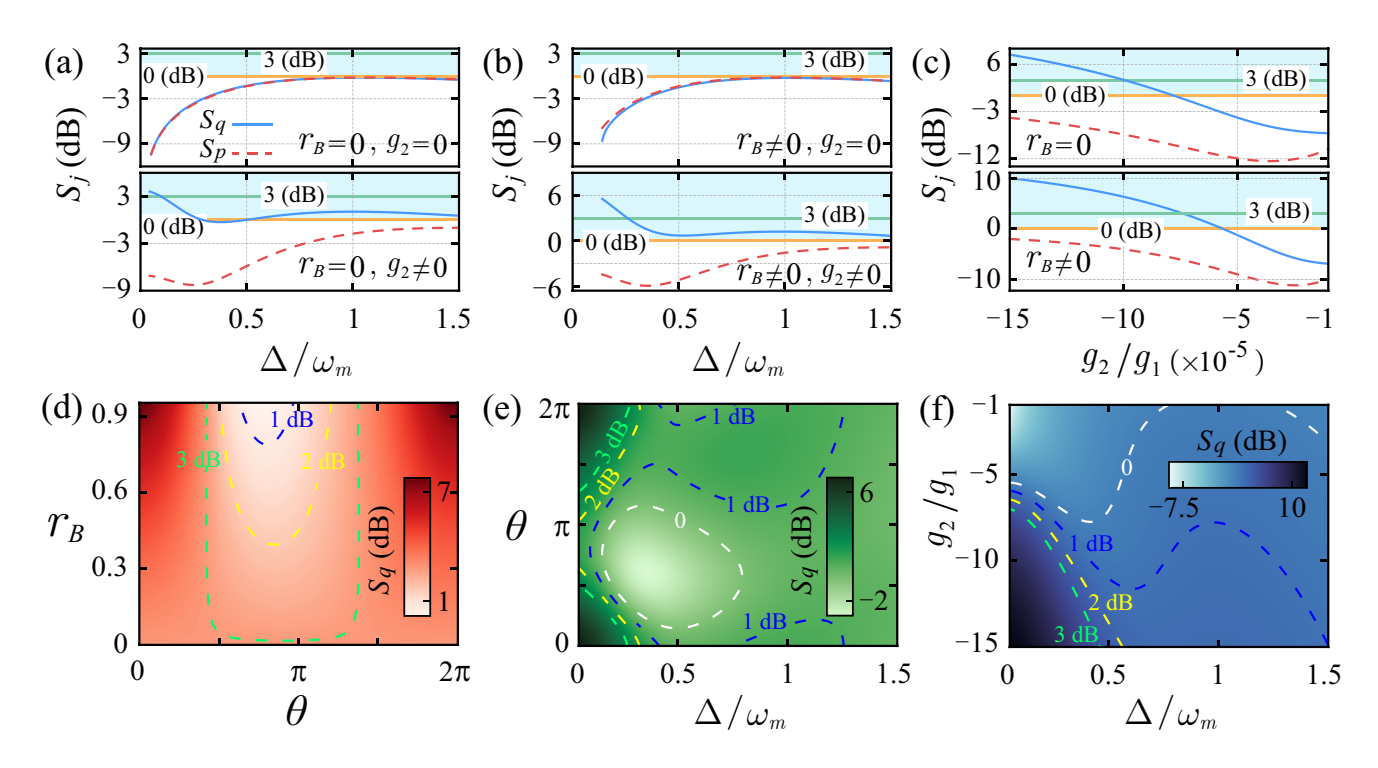


FIG. 4. Enhancement of mechanical squeezing via the synergistic effect of QOC and coherent feedback. The mechanical quadrature squeezing degree  $S_j$  versus the scaled optical detuning  $\Delta/\omega_m$ : (a) in the absence of coherent feedback ( $r_B=0$ ) with  $g_2/g_1=0$  (top panel) and  $g_2/g_1=-10^{-3}$  (bottom panel); (b) in the presence of coherent feedback ( $r_B=0.8, \theta=0$ ) with  $g_2/g_1=0$  (top panel) and  $g_2/g_1=-10^{-3}$  (bottom panel). (c) The mechanical quadrature squeezing degree  $S_j$  as a function of dimensionless QOC strength  $g_2/g_1$  for  $\Delta/\omega_m=0.1$  with  $r_B=0$  (top panel) and  $r_B=0.8, \theta=0$  (bottom panel). The blue solid and red dashed lines correspond to  $S_q$  and  $S_p$ , respectively. (d-f) The Q-quadrature squeezing degree  $S_q$  under different parameter settings: (d) as a function of the reflection coefficient  $r_B$  and optical phase shift  $\theta$  with  $\Delta/\omega_m=0.1$  and  $g_2/g_1=-10^{-3}$ ; (e) as a function of the scaled optical detuning  $\Delta/\omega_m$  and optical phase shift  $\theta$  with  $r_B=0.8$  and  $r_B=0.8$  an

the zero-point fluctuation of the membrane motion.  $S_j>0$  indicates that the fluctuation of the j quadrature is squeezed. In Particular,  $S_j>3$  corresponds to a 50% reduction of noise below the zero-point fluctuation, i.e.,  $\sigma_j<\sigma_{\rm zpf}/2$ , which is regarded as strong mechanical squeezing beyond the 3dB limit

In Figs. 4(a) and 4(b), we present the squeezing degrees  $S_q$ and  $S_p$  as functions of the scaled optical detuning  $\Delta/\omega_m$  for different reflection coefficients  $r_B$  and dimensionless QOC strengths  $g_2/g_1$ . The results highlight the distinct roles of QOC and coherent feedback. Specifically, in the absence of QOC  $(g_2/g_1 = 0)$ , no mechanical squeezing is present  $(S_q < 0 \text{ and } S_p < 0)$ , regardless of whether coherent feedback is applied. In contrast, for  $g_2/g_1 \neq 0$ , the fluctuation of the q quadrature exhibits squeezing ( $S_q>0$ ), and even without feedback ( $r_B=0$ ), the 3dB limit of squeezing can be beaten, with  $S_q > 3$  over a finite range of detuning  $\Delta$ . The presence of feedback  $(r_B \neq 0)$  could further enhance the squeezing degree and broaden the accessible detuning range. To further present the crucial role of QOC, we show the behavior of  $S_q$  versus dimensionless QOC strength  $g_2/g_1$  for different reflection coefficients  $r_B$  in the vicinity of  $\Delta/\omega_m = 0.1$  in Fig. 4(c). As is seen, for the negative sign of QOC,  $S_q$  can exceed the 3dB limit in a broad parameter region, and the incor-

poration of feedback  $(r_B \neq 0)$  leads to a substantial increase in  $S_q$ . Notably, it is also confirmed that for the positive sign of QOC, mechanical squeezing is unachievable in both quadratures with  $S_q < 0$  and  $S_p < 0$ . These results suggest that for mechanical squeezing generation, negative QOC serves as an essential fundamental resource, whereas feedback provides an effective means to enhance the squeezing degree. To support this observation, we further show the dependence of mechanical squeezing degree  $S_q$  on the QOC and feedback controlling parameters in Figs. 4(d)-4(f). It is seen that the mechanical squeezing degree  $S_q$  increases monotonically with both  $r_B$ and  $g_2/g_1$ , and exhibits a periodic dependence on the optical phase shift  $\theta$  with a period of  $2\pi$ , reaching its maximum at  $\theta = 0$  and minimum at  $\theta = \pi$ . Particularly, for  $r_B = 0.8$  and  $\theta=0$ , the optimal mechanical squeezing can be above  $10\mathrm{dB}$ in the vicinity of  $g_2/g_1 = -15 \times 10^{-3}$ . Evidently, this variation behavior of mechanical squeezing is similar to that of the COM entanglement with such QOC and feedback controlling parameters as discussed in the previous section.

### V. CONCLUSION

In summary, we have investigated the synergistic effects of QOC and coherent feedback on the generation and manipulation of COM entanglement and mechanical squeezing. Specifically, we consider here a membrane-embedded COM system coupled with a coherent feedback loop, in which the membrane interacts with the cavity mode through both linear and quadratic optomechanical couplings. This hybrid architecture offers two critical advantages over a bare COM system in terms of parameter tunability: (i) the incorporation of QOC provides a flexible means to tune the frequency of the membrane, where the sign of QOC determines whether the mechanical mode becomes stiffer or softer; (ii) feeding the output field back into the cavity effectively reduces the cavity decay rate. Thanks to these advantageous features, we show that COM entanglement can be considerably enhanced for positive QOC strength and suitable feedback parameters. This enhancement originates from the relaxed stability conditions of the COM system and the suppression of cavity decay enabled by the synergistic control of QOC and coherent feedback. More interestingly, for generating mechanical squeezing, we find that introducing negative QOC to COM system offers a viable route without the use of sophisticated techniques like backaction-evading measurements [39-41] or reservoir engineering [45–47]. Meanwhile, the further application of coherent feedback could enhance the squeezing degree and broaden the accessible parameter range. With suitable QOC and feedback parameters, we show that strong mechanical squeezing beyond the 3dB limit is achieved, reaching values above 10dB. This work opens up a promising route for nonclassical states preparation [53–61] with COM devices through exploiting the synergistic effects of QOC and coherent feedback. This is expected to be extendable to diverse hybrid COM platforms, such as those based on microwave electromechanical resonator [70, 72–75], optical [71] or photonic crystal [69, 76] cavities, and nanoparticle-on-mirror structures [92].

#### VI. ACKNOWLEDGMENT

H.J. is supported by the National Key R&D Program of China (Grants No. 2024YFE0102400), the National Natural Science Foundation of China (NSFC, Grants No. 11935006, 12421005), and the Hunan Provincial Major Sci-Tech Program (Grant No. 2023ZJ1010). L.-M.K. is supported by the NSFC (Grants No. 12247105, 11935006, 12175060 and 12421005), the Hunan Provincial Major Sci-Tech Program (Grant No. 2023ZJ1010), and the Henan Science and Technology Major Project (Grant No. 241100210400). Y.-F.J. is supported by the NSFC (Grant No. 12405029) and the Natural Science Foundation of Henan Province (Grant No. 252300421221). H.Z. is supported by the Natural Science Foundation of Henan Province (Grants No. 252300421794, 242300420665) and the Doctoral Research Foundation of Zhengzhou University of Light Industry (Grant No. 2022BSJJZK20). Y.-C.L. is supported by the NSFC (Grant No. 12304474) and the Natural Science Foundation of Henan Province (Grant No. 252300421222). Y.W. is supported by the NSFC (Grant No. 12205256) and the Henan Provincial Science and Technology Research Project (Grant No. 232102221001).

<sup>[1]</sup> R. Horodecki, P. Horodecki, M. Horodecki, and K. Horodecki, Quantum entanglement, Rev. Mod. Phys. 81, 865 (2009).

<sup>[2]</sup> U. L. Andersen, T. Gehring, C. Marquardt, and G. Leuchs, 30 years of squeezed light generation, Phys. Scr. **91**, 053001 (2016).

<sup>[3]</sup> J. P. Dowling and G. J. Milburn, Quantum technology: the second quantum revolution, Phil. Trans. R. Soc. A 361, 1655 (2003).

<sup>[4]</sup> S. L. Braunstein and P. van Loock, Quantum information with continuous variables, Rev. Mod. Phys. 77, 513 (2005).

<sup>[5]</sup> U. L. Andersen, G. Leuchs, and C. Silberhorn, Continuous-variable quantum information processing, Laser & Photon. Rev. 4, 337 (2010).

<sup>[6]</sup> K. Modi, A. Brodutch, H. Cable, T. Paterek, and V. Vedral, The classical-quantum boundary for correlations: Discord and related measures, Rev. Mod. Phys. 84, 1655 (2012).

<sup>[7]</sup> Y. Xia, A. R. R. Agrawal, C. M. M. Pluchar, A. J. J. Brady, Z. Liu, Q. Zhuang, D. J. J. Wilson, and Z. Zhang, Entanglement-enhanced optomechanical sensing, Nat. Photon. 17, 470 (2023).

<sup>[8]</sup> Q.-Y. He, L. Rosales-Zárate, G. Adesso, and M. D. Reid, Secure Continuous Variable Teleportation and Einstein-Podolsky-Rosen Steering, Phys. Rev. Lett. 115, 180502 (2015).

<sup>[9]</sup> X. Zhang, H.-O. Li, G. Cao, M. Xiao, G.-C. Guo, and G.-P. Guo, Semiconductor quantum computation, Natl. Sci. Rev. 6, 32 (2018).

<sup>[10]</sup> X.-L. Wang, L.-K. Chen, W. Li, H.-L. Huang, C. Liu, C. Chen, Y.-H. Luo, Z.-E. Su, D. Wu, Z.-D. Li, H. Lu, Y. Hu, X. Jiang, C.-Z. Peng, L. Li, N.-L. Liu, Y.-A. Chen, C.-Y. Lu, and J.-W. Pan, Experimental Ten-Photon Entanglement, Phys. Rev. Lett. 117, 210502 (2016).

<sup>[11]</sup> H.-N. Dai, B. Yang, A. Reingruber, X.-F. Xu, X. Jiang, Y.-A. Chen, Z.-S. Yuan, and J.-W. Pan, Generation and detection of atomic spin entanglement in optical lattices, Nat. Phys. 12, 783 (2016).

<sup>[12]</sup> X.-Y. Luo, Y. Yu, J.-L. Liu, M.-Y. Zheng, C.-Y. Wang, B. Wang, J. Li, X. Jiang, X.-P. Xie, Q. Zhang, X.-H. Bao, and J.-W. Pan, Postselected Entanglement between Two Atomic Ensembles Separated by 12.5 km, Phys. Rev. Lett. 129, 050503 (2022).

<sup>[13]</sup> J. Ma, X. Wang, C. Sun, and F. Nori, Quantum spin squeezing, Phys. Rep. 509, 89 (2011).

<sup>[14]</sup> J. Estève, C. Gross, A. Weller, S. Giovanazzi, and M. K. Oberthaler, Squeezing and entanglement in a Bose-Einstein condensate, Nature (London) 455, 1216 (2008).

<sup>[15]</sup> T. P. Purdy, P.-L. Yu, R. W. Peterson, N. S. Kampel, and C. A. Regal, Strong Optomechanical Squeezing of Light, Phys. Rev. X 3, 031012 (2013).

- [16] Y.-D. Wang and A. A. Clerk, Reservoir-Engineered Entanglement in Optomechanical Systems, Phys. Rev. Lett. 110, 253601 (2013).
- [17] Y.-F. Jiao, Y.-L. Zuo, Y. Wang, W. Lu, J.-Q. Liao, L.-M. Kuang, and H. Jing, Tripartite Quantum Entanglement with Squeezed Optomechanics, Laser & Photon. Rev. 18, 2301154.
- [18] Y.-F. Jiao, J. Wang, D.-Y. Wang, L. Tang, Y. Wang, Y.-L. Zuo, W.-S. Bao, L.-M. Kuang, and H. Jing, Phase-selective tripartite entanglement and asymmetric Einstein-Podolsky-Rosen steering in squeezed optomechanics, Phys. Rev. A 112, 012421 (2025).
- [19] D.-G. Lai, J.-Q. Liao, A. Miranowicz, and F. Nori, Noise-Tolerant Optomechanical Entanglement via Synthetic Magnetism, Phys. Rev. Lett. 129, 063602 (2022).
- [20] J.-X. Liu, Y.-F. Jiao, Y. Li, X.-W. Xu, Q.-Y. He, and H. Jing, Phase-Controlled Asymmetric Optomechanical Entanglement against Optical Backscattering, Sci. China-Phys. Mech. Astron. 66, 230312 (2023).
- [21] J.-X. Liu, J.-Y. Yang, T.-X. Lu, Y.-F. Jiao, and H. Jing, Phase-controlled robust quantum entanglement of remote mechanical oscillators, Phys. Rev. A 109, 023519 (2024).
- [22] D.-G. Lai, Y.-H. Chen, W. Qin, A. Miranowicz, and F. Nori, Tripartite optomechanical entanglement via optical-dark-mode control, Phys. Rev. Res. 4, 033112 (2022).
- [23] J. Huang, D.-G. Lai, and J.-Q. Liao, Thermal-noise-resistant optomechanical entanglement via general dark-mode control, Phys. Rev. A 106, 063506 (2022).
- [24] D. Riste, M. Dukalski, C. A. Watson, G. de Lange, M. J. Tiggelman, Y. M. Blanter, K. W. Lehnert, R. N. Schouten, and L. Di-Carlo, Deterministic entanglement of superconducting qubits by parity measurement and feedback, Nature (London) 502, 350 (2013).
- [25] J. Li, G. Li, S. Zippilli, D. Vitali, and T. Zhang, Enhanced entanglement of two different mechanical resonators via coherent feedback, Phys. Rev. A 95, 043819 (2017).
- [26] D. Miki, N. Matsumoto, A. Matsumura, T. Shichijo, Y. Sugiyama, K. Yamamoto, and N. Yamamoto, Generating quantum entanglement between macroscopic objects with continuous measurement and feedback control, Phys. Rev. A 107, 032410 (2023).
- [27] M. Ho, E. Oudot, J.-D. Bancal, and N. Sangouard, Witnessing Optomechanical Entanglement with Photon Counting, Phys. Rev. Lett. **121**, 023602 (2018).
- [28] M. Wang, X.-Y. Lü, Y.-D. Wang, J. Q. You, and Y. Wu, Macroscopic Quantum Entanglement in Modulated Optomechanics, Phys. Rev. A 94, 053807 (2016).
- [29] C.-S. Hu, L.-T. Shen, Z.-B. Yang, H. Wu, Y. Li, and S.-B. Zheng, Manifestation of Classical Nonlinear Dynamics in Optomechanical Entanglement with a Parametric Amplifier, Phys. Rev. A 100, 043824 (2019).
- [30] J. Yang, T.-X. Lu, M. Peng, J. Liu, Y.-F. Jiao, and H. Jing, Multi-field-driven optomechanical entanglement, Opt. Express 32, 785 (2024).
- [31] Y.-F. Jiao, S.-D. Zhang, Y.-L. Zhang, A. Miranowicz, L.-M. Kuang, and H. Jing, Nonreciprocal Optomechanical Entanglement against Backscattering Losses, Phys. Rev. Lett. 125, 143605 (2020).
- [32] Y.-F. Jiao, J.-X. Liu, Y. Li, R. Yang, L.-M. Kuang, and H. Jing, Nonreciprocal Enhancement of Remote Entanglement between Nonidentical Mechanical Oscillators, Phys. Rev. Applied 18, 064008 (2022).
- [33] Y.-F. Jiao, J. Wang, Q. Zhang, H. Lin, and H. Jing, Nonreciprocal quantum optics: New effects and applications in quantum sensing, Fundamental Research

- https://doi.org/10.1016/j.fmre.2024.12.018 (2025).
- [34] A. Mari and J. Eisert, Gently Modulating Optomechanical Systems, Phys. Rev. Lett. **103**, 213603 (2009).
- [35] X. Han, D.-Y. Wang, C.-H. Bai, W.-X. Cui, S. Zhang, and H.-F. Wang, Mechanical squeezing beyond resolved sideband and weak-coupling limits with frequency modulation, Phys. Rev. A 100, 033812 (2019).
- [36] F. Yang, M. Fu, B. Bosnjak, R. H. Blick, Y. Jiang, and E. Scheer, Mechanically Modulated Sideband and Squeezing Effects of Membrane Resonators, Phys. Rev. Lett. 127, 184301 (2021).
- [37] X.-Y. Lü, J.-Q. Liao, L. Tian, and F. Nori, Steady-state mechanical squeezing in an optomechanical system via Duffing nonlinearity, Phys. Rev. A 91, 013834 (2015).
- [38] S. Huang and A. Chen, Mechanical squeezing in a dissipative optomechanical system with two driving tones, Phys. Rev. A 103, 023501 (2021).
- [39] R. Ruskov, K. Schwab, and A. N. Korotkov, Squeezing of a nanomechanical resonator by quantum nondemolition measurement and feedback, Phys. Rev. B 71, 235407 (2005).
- [40] A. Szorkovszky, A. C. Doherty, G. I. Harris, and W. P. Bowen, Mechanical Squeezing via Parametric Amplification and Weak Measurement, Phys. Rev. Lett. 107, 213603 (2011).
- [41] A. Szorkovszky, G. A. Brawley, A. C. Doherty, and W. P. Bowen, Strong thermomechanical squeezing via weak measurement, Phys. Rev. Lett. 110, 184301 (2013).
- [42] J. Huang, D.-G. Lai, and J.-Q. Liao, Controllable generation of mechanical quadrature squeezing via dark-mode engineering in cavity optomechanics, Phys. Rev. A 108, 013516 (2023).
- [43] J. Zhang, Y.-X. Liu, and F. Nori, Cooling and squeezing the fluctuations of a nanomechanical beam by indirect quantum feedback control, Phys. Rev. A 79, 052102 (2009).
- [44] A. Vinante and P. Falferi, Feedback-Enhanced Parametric Squeezing of Mechanical Motion, Phys. Rev. Lett. 111, 207203 (2013).
- [45] P. Rabl, A. Shnirman, and P. Zoller, Generation of squeezed states of nanomechanical resonators by reservoir engineering, Phys. Rev. B 70, 205304 (2004).
- [46] M. J. Woolley and A. A. Clerk, Two-mode squeezed states in cavity optomechanics via engineering of a single reservoir, Phys. Rev. A 89, 063805 (2014).
- [47] S.-Y. Bai and J.-H. An, Generating Stable Spin Squeezing by Squeezed-Reservoir Engineering, Phys. Rev. Lett. 127, 083602 (2021).
- [48] M. Aspelmeyer, T. J. Kippenberg, and F. Marquardt, Cavity optomechanics, Rev. Mod. Phys. 86, 1391 (2014).
- [49] T. Rocheleau, T. Ndukum, C. Macklin, J. Hertzberg, A. Clerk, and K. Schwab, Preparation and detection of a mechanical resonator near the ground state of motion, Nature (London) 463, 72 (2010).
- [50] A. D. O'Connell, M. Hofheinz, M. Ansmann, R. C. Bialczak, M. Lenander, E. Lucero, M. Neeley, D. Sank, H. Wang, M. Weides, J. Wenner, J. M. Martinis, and A. N. Cleland, Quantum ground state and single-phonon control of a mechanical resonator, Nature (London) 464, 697 (2010).
- [51] L. Du, J. Monsel, W. Wieczorek, and J. Splettstoesser, Coherent feedback control for cavity optomechanical systems with a frequency-dependent mirror, Phys. Rev. A 111, 013506 (2025).
- [52] H. Xiong, L.-G. Si, X.-Y. Lü, X.-X. Yang, and Y. Wu, Review of cavity optomechanics in the weak-coupling regime: from linearization to intrinsic nonlinear interactions, Sci. China Phys. Mech. Astron. 58, 1 (2015).
- [53] P. Rabl, Photon Blockade Effect in Optomechanical Systems, Phys. Rev. Lett. 107, 063601 (2011).

- [54] C. Zhai, R. Huang, H. Jing, and L.-M. Kuang, Mechanical switch of photon blockade and photon-induced tunneling, Opt. Express 27, 27649 (2019).
- [55] H. Xie, C.-G. Liao, X. Shang, M.-Y. Ye, and X.-M. Lin, Phonon blockade in a quadratically coupled optomechanical system, Phys. Rev. A 96, 013861 (2017).
- [56] L.-L. Zheng, T.-S. Yin, Q. Bin, X.-Y. Lü, and Y. Wu, Single-photon-induced phonon blockade in a hybrid spinoptomechanical system, Phys. Rev. A 99, 013804 (2019).
- [57] X.-Y. Lü, L.-L. Zheng, G.-L. Zhu, and Y. Wu, Single-Photon-Triggered Quantum Phase Transition, Phys. Rev. Applied 9, 064006 (2018).
- [58] G.-L. Zhu, X.-Y. Lü, L.-L. Zheng, Z.-M. Zhan, F. Nori, and Y. Wu, Single-photon-triggered quantum chaos, Phys. Rev. A 100, 023825 (2019).
- [59] J. I. Cirac, P. Zoller, H. J. Kimble, and H. Mabuchi, Quantum State Transfer and Entanglement Distribution among Distant Nodes in a Quantum Network, Phys. Rev. Lett. 78, 3221 (1997).
- [60] T. A. Palomaki, J. W. Harlow, J. D. Teufel, R. W. Simmonds, and K. W. Lehnert, Coherent state transfer between itinerant microwave fields and a mechanical oscillator, Nature (London) 495, 210 (2013).
- [61] I. Marinković, A. Wallucks, R. Riedinger, S. Hong, M. Aspelmeyer, and S. Gröblacher, Optomechanical Bell Test, Phys. Rev. Lett. 121, 220404 (2018).
- [62] H. Yu, L. McCuller, M. Tse, N. Kijbunchoo, L. Barsotti, N. Mavalvala, and L. S. Collaboration, Quantum correlations between light and the kilogram-mass mirrors of LIGO, Nature (London) 583, 43 (2020).
- [63] D. Vitali, S. Gigan, A. Ferreira, H. R. Böhm, P. Tombesi, A. Guerreiro, V. Vedral, A. Zeilinger, and M. Aspelmeyer, Optomechanical Entanglement between a Movable Mirror and a Cavity Field, Phys. Rev. Lett. 98, 030405 (2007).
- [64] C. Genes, A. Mari, P. Tombesi, and D. Vitali, Robust Entanglement of a Micromechanical Resonator with Output Optical Fields, Phys. Rev. A 78, 032316 (2008).
- [65] R. Ghobadi, S. Kumar, B. Pepper, D. Bouwmeester, A. I. Lvovsky, and C. Simon, Optomechanical Micro-Macro Entanglement, Phys. Rev. Lett. 112, 080503 (2014).
- [66] E. E. Wollman, C. U. Lei, A. J. Weinstein, J. Suh, A. Kronwald, F. Marquardt, A. A. Clerk, and K. C. Schwab, Quantum squeezing of motion in a mechanical resonator, Science 349, 952 (2015).
- [67] G. S. Agarwal and S. Huang, Strong mechanical squeezing and its detection, Phys. Rev. A 93, 043844 (2016).
- [68] S. Marti, U. von Lupke, O. Joshi, Y. Yang, M. Bild, A. Omahen, Y. Chu, and M. Fadel, Quantum squeezing in a nonlinear mechanical oscillator, Nat. Phys. 20, 1448 (2024).
- [69] R. Riedinger, S. Hong, R. A. Norte, J. A. Slater, J. Shang, A. G. Krause, V. Anant, M. Aspelmeyer, and S. Gröblacher, Non-classical correlations between single photons and phonons from a mechanical oscillator, Nature (London) 530, 313 (2016).
- [70] T. A. Palomaki, J. D. Teufel, R. W. Simmonds, and K. W. Lehnert, Entangling Mechanical Motion with Microwave Fields, Science 342, 710 (2013).
- [71] J. Chen, M. Rossi, D. Mason, and A. Schliesser, Entanglement of propagating optical modes via a mechanical interface, Nat. Commun. 11, 943 (2020).
- [72] S. Barzanjeh, E. S. Redchenko, M. Peruzzo, M. Wulf, D. P. Lewis, G. Arnold, and J. M. Fink, Stationary entangled radiation from micromechanical motion, Nature (London) 570, 480 (2019).
- [73] C. F. Ockeloen-Korppi, E. Damskägg, J.-M. Pirkkalainen, M. Asjad, A. A. Clerk, F. Massel, M. J. Woolley, and M. A.

- Sillanpää, Stabilized entanglement of massive mechanical oscillators, Nature (London) **556**, 478 (2018).
- [74] S. Kotler, G. A. Peterson, E. Shojaee, F. Lecocq, K. Cicak, A. Kwiatkowski, S. Geller, S. Glancy, E. Knill, R. W. Simmonds, J. Aumentado, and J. D. Teufel, Direct observation of deterministic macroscopic entanglement, Science 372, 622 (2021).
- [75] L. Mercier de Lépinay, C. F. Ockeloen-Korppi, M. J. Woolley, and M. A. Sillanpää, Quantum mechanics–free subsystem with mechanical oscillators, Science 372, 625 (2021).
- [76] R. Riedinger, A. Wallucks, I. Marinković, C. Löschnauer, M. Aspelmeyer, S. Hong, and S. Gröblacher, Remote quantum entanglement between two micromechanical oscillators, Nature (London) 556, 473 (2018).
- [77] R. Dassonneville, R. Assouly, T. Peronnin, A. Clerk, A. Bienfait, and B. Huard, Dissipative Stabilization of Squeezing Beyond 3 dB in a Microwave Mode, PRX Quantum 2, 020323 (2021).
- [78] W. Qin, A. Miranowicz, and F. Nori, Beating the 3 dB Limit for Intracavity Squeezing and Its Application to Nondemolition Qubit Readout, Phys. Rev. Lett. 129, 123602 (2022).
- [79] K. Kustura, C. Gonzalez-Ballestero, A. d. l. R. Sommer, N. Meyer, R. Quidant, and O. Romero-Isart, Mechanical Squeezing via Unstable Dynamics in a Microcavity, Phys. Rev. Lett. 128, 143601 (2022).
- [80] C. U. Lei, A. J. Weinstein, J. Suh, E. E. Wollman, A. Kronwald, F. Marquardt, A. A. Clerk, and K. C. Schwab, Quantum Nondemolition Measurement of a Quantum Squeezed State Beyond the 3 dB Limit, Phys. Rev. Lett. 117, 100801 (2016).
- [81] W. Jia, V. Xu, K. Kuns, M. Nakano, L. Barsotti, M. Evans, N. Mavalvala, and L. S. Collaboration, Squeezing the quantum noise of a gravitational-wave detector below the standard quantum limit, Science 385, 1318 (2024).
- [82] M. Kamba, N. Hara, and K. Aikawa, Quantum squeezing of a levitated nanomechanical oscillator, Science 389, 1225 (2025).
- [83] L. Zhang and Z. Song, Modification on static responses of a nano-oscillator by quadratic optomechanical couplings, Sci. China-Phys. Mech. Astron. 57, 880 (2014).
- [84] A. Xuereb and M. Paternostro, Selectable linear or quadratic coupling in an optomechanical system, Phys. Rev. A 87, 023830 (2013).
- [85] L. Zhang and H.-Y. Kong, Self-sustained oscillation and harmonic generation in optomechanical systems with quadratic couplings, Phys. Rev. A 89, 023847 (2014).
- [86] M. Bhattacharya, H. Uys, and P. Meystre, Optomechanical trapping and cooling of partially reflective mirrors, Phys. Rev. A 77, 033819 (2008).
- [87] C. W. Gardiner and P. Zoller, *Quantum Noise* (Springer, Berlin, 2000).
- [88] G. S. Agarwal, *Quantum optics* (Cambridge University Press, Cambridge, UK, 2013).
- [89] G. Adesso, A. Serafini, and F. Illuminati, Extremal entanglement and mixedness in continuous variable systems, Phys. Rev. A 70, 022318 (2004).
- [90] N. Ghorbani, A. Motazedifard, and M. H. Naderi, Effects of quadratic optomechanical coupling on bipartite entanglements, mechanical ground-state cooling, and mechanical quadrature squeezing in an electro-optomechanical system, Phys. Rev. A 111, 013524 (2025).
- [91] R. Zhang, Y. Fang, Y.-Y. Wang, S. Chesi, and Y.-D. Wang, Strong mechanical squeezing in an unresolved-sideband optomechanical system, Phys. Rev. A 99, 043805 (2019).
- [92] H.-Y. Yu, Y.-F. Jiao, J. Wang, F. Li, B. Yin, T. Jiang, Q.-R. Liu, H. Jing, and K. Wei, Strong Molecule-Light Entanglement with

Molecular Cavity Optomechanics, arXiv:2505.21227.